EI SEVIER

Contents lists available at ScienceDirect

### Smart Agricultural Technology

journal homepage: www.journals.elsevier.com/smart-agricultural-technology





## A support vector machine and image processing based approach for counting open cotton bolls and estimating lint yield from UAV imagery

Arun Bawa <sup>a,b</sup>, Sayantan Samanta <sup>c</sup>, Sushil Kumar Himanshu <sup>b,d</sup>, Jasdeep Singh <sup>b,e</sup>, JungJin Kim <sup>b,f</sup>, Tian Zhang <sup>b,g</sup>, Anjin Chang <sup>h</sup>, Jinha Jung <sup>i</sup>, Paul DeLaune <sup>b</sup>, James Bordovsky <sup>j</sup>, Edward Barnes <sup>k</sup>, Srinivasulu Ale <sup>b,\*</sup>

- <sup>a</sup> Texas A&M AgriLife Blackland Research and Extension Center (Texas A&M University System), Temple, TX, USA
- b Texas A&M AgriLife Research (Texas A&M University System), Vernon, TX, USA
- <sup>c</sup> Water Management and Hydrologic Sciences Program, Texas A&M University, College Station, TX, USA
- d Department of Food, Agriculture and Bioresources, Asian Institute of Technology, Khlong Luang, Thailand
- e Department of Crop Sciences, University of Illinois Urbana-Champaign, Urbana, IL, USA
- f Seoul National University of Science and Technology, Seoul, South Korea
- g Department of Natural Resources Ecology and Management, Oklahoma State University, Stillwater, OK, USA
- h Advanta Seeds, Amarillo, TX, USA
- <sup>1</sup> Lyles School of Civil Engineering, Purdue University, West Lafayette, IN, USA
- <sup>j</sup> Texas A&M AgriLife Research Station, Halfway, TX, USA
- k Cotton Incorporated, Cary, NC, USA

#### ARTICLEINFO

# Keywords: Machine learning Supervised classification Remote sensing Phenotyping Otsu thresholding

#### ABSTRACT

Cotton boll count is an important phenotypic trait that aids in a better understanding of the genetic and physiological mechanisms of cotton growth. Several computer vision technologies are available for cotton boll segmentation. However, estimating the number of cotton bolls in a segmented cluster of cotton bolls is a challenging task due to the complex shapes of cotton bolls. This study proposed a combination of spectral-spatial and supervised machine learning based methods for cotton boll candidate recognition and counting from high resolution RGB images obtained from unmanned aerial vehicles (UAVs). An algorithm consisting of machine vision, band-mean filter, Otsu thresholding, red/blue band ratio filter, and geometrical characteristics-based error removal techniques, was employed to detect open cotton boll pixels under several environmental settings. In addition, a support vector machine (SVM) based encoding method was developed using geometric features of cotton boll candidates to predict the number of cotton bolls from the segmented cotton boll candidates. This algorithm was implemented over three experiment sites with three cotton varieties, two tillage practices, seven cover crop treatments, two irrigation regimes (irrigated and rainfed), 26 irrigation levels, and two sensors (DJI FC6310 RGB and MicaSense Rededge) capturing images at two spatial resolutions (0.75 cm and 1.07 cm) over two growing seasons (2019 and 2021). These different experimental settings allowed the proposed approaches to be validated against a variety of complex backgrounds. A visual inspection of 1000 randomly selected pixels revealed that the proposed cotton boll candidate recognition approach was highly effective in segmenting cotton bolls and background pixels, with high classification accuracy (> 95%) and a low number of falsely classified pixels (precision > 0.96; recall > 0.93). A high correlation between ground truth observations and predicted cotton boll count indicated that the use of geometric features of segmented candidates as predictors in association with the SVM model demonstrated a good performance in estimating boll count from recognized cotton boll candidates. Furthermore, linear regression analyses revealed that both boll count and candidate area are potential predictors of lint yield, with boll count being a better predictor than candidate area. Overall, the study demonstrated that machine vision/learning techniques can be potentially used on UAV images to count the number of cotton bolls and predict lint yield over large acreages with reasonable accuracy.

E-mail address: sriniale@ag.tamu.edu (S. Ale).

https://doi.org/10.1016/j.atech.2022.100140

<sup>\*</sup> Corresponding author.

#### 1. Introduction

Cotton boll count is a valuable phenotypic trait, which most cotton breeders and producers use to develop a thorough understanding of the physiological and genetic crop growth [23]. Boll count also provides a means to assess crop growth conditions and facilitate timely crop management decisions to prevent yield losses. Cotton boll count is also an indicator of lint yield. Wells and Meredith [25] reported a positive correlation between bolls per unit area and lint yield. Yeom et al. [27] related area under boll pixels with cotton yield and reported a high correlation ( $R^2 = 0.65$ ). Rouze et al. [18] reported a moderate correlation ( $R^2 = 0.49$ ) between open boll count and cotton yield. Therefore, boll count can also serve as an important parameter for yield estimation and in gene-selection in plant breeding studies [8,25]. In addition, yield mapping using precision agriculture tools, can assist growers in overcoming in-field spatial variability [12].

Traditional boll counting methods are based on manual sampling and visual inspection, which are error-prone and also impractical for high acreage plant breeding programs [23]. With the technological advent of the Global Positioning System (GPS) integrated sensors in agriculture, it is now possible to monitor crop growth in real-time and automate farming operations [22,29]. A few studies were conducted over the last decade to automate cotton boll pixel extraction using remote electromagnetic radiation sensors mounted on Unmanned Aerial Vehicles (UAVs) or agri-robots. For example, using multispectral aerial imagery, Yeom et al. [27] proposed a region growing and Otsu threshold [16] based cotton boll pixel recognition method with high classification accuracy. Rouze et al. [18] generated open boll maps using a threshold for red/blue band ratio. Jung et al. [11] detected cotton bolls using a threshold of 190 for the red band in an 8-bit image. Although these studies have provided potential solutions for the segmentation of cotton boll pixels from the background, the segmented cotton boll pixels results in clusters of cotton bolls and none of the above mentioned study investigated the estimation of a number of cotton bolls from the detected cotton boll clusters. Sun et al. [23] proposed three geometric-based algorithms for cotton boll counting from high spatial resolution measurements from an agri-robot, but a similar study for UAV imagery was not found in the literature. Additionally, Sun et al. [23] boll counting method cannot be applied with UAV imagery due to the coarser spatial resolution of UAV measurements (a few cm) as compared to agri-robot measurements (< 1 mm). The UAV detected cotton boll clusters can have varied and complex shapes, mainly because of the cotton boll face orientation relative to the UAV sensor. Hence, simple area or size filters can not be applied to separate cotton bolls from the detected boll clusters. In this study, a novel approach was introduced to estimate the number of open cotton bolls from a red-green-blue (RGB) aerial imagery while segregating cotton boll pixels from the image background.

Agricultural scientists are interested in rapidly collecting and analyzing a greater volume of high quality phenotypic trait data for crop improvement through breeding or other site-specific precision-agriculture approaches [20,22]. Because of their high spatio-temporal resolution, relatively lower operational cost, and less complexity in the data collection [20,29], UAVs have emerged as an intriguing remote sensing option for precision farming and agronomic research [19,29]. In addition, data science tools such as machine learning (ML) methods (e.g., support vector and random forests) are frequently used to extract information from the UAV imageries [17,28]. Such tools can be used in agricultural applications when classifying objects with complex and varied structures. For example, Yamamoto et al. [26] used X-means clustering algorithm to detect tomatoes and Li et al. [14] adopted random forest to achieve semantic labeling prediction for in-field cotton detection from images. These tools have the potential to automate the whole process, and hence they can be used in the development of decision support tools.

In machine learning, support vector machines (SVMs) are highdimensional hyperplane-based pattern recognition learning models that are used for the classification and regression analysis [4,7]. Due to SVMs' capability to model complicated non-linear relationships, they are preferred over conventional classification and regression techniques such as logistic regression and linear or multiple regression models [13]. Varying sizes, complex shapes, orientation, and overlapping of cotton bolls along with a lack of linear relation between detected cotton boll candidate size and boll count, make cotton boll counting from UAV images a substantially challenging task. Therefore, the overall goal of this study was to evaluate an SVM regression (SVR)-based approach to establish non-linear relations among detected cotton boll clusters and cotton boll count across diverse environmental settings. Specific objectives of the study were to: (1) develop a simplified method for cotton boll candidate recognition from an image captured by an RGB sensor, (2) develop and validate an SVR-based method for counting cotton bolls within recognized cotton boll candidates, and (3) estimate cotton yield as a function of boll count and area under recognized boll candidates.

#### 2. Materials and methods

#### 2.1. Experiment setup

In this study, UAV measurements were made over 161 plots from three cotton experimental sites. Of these, two sites (I and II) are located at the Texas A&M AgriLife Research Station (34°15′ N, 99°30′ W), Chillicothe, Texas. The UAV measurements from these sites were collected during the 2021 cotton growing season. Experiment site I consisted of 12 irrigated plots (4 cover crop treatments X 3 replications) and experiment site II consisted of 21 dryland plots (7 cover crop treatments X 3 replications). The PHY 480 cultivar was used at both sites. More details about these field experiments can be found in DeLaune et al. [6] and DeLaune and Mubvumba [5]. These two cover crop experiments provided an opportunity to validate the approaches developed for cotton boll candidate recognition and boll count estimation across a variety of complex backgrounds.

At the Texas A&M AgriLife Research Station (34°10′ N, 101°56′ W), Halfway, Texas experiment site (Site III), UAV images were collected from a cotton irrigation water use efficiency experiment. More details about the Halfway field experiment can be found in Bordovsky et al. [2], Himanshu et al. [10], and Himanshu et al. [9]. The UAV measurements from this experiment allowed the validation of developed approaches against UAV images collected using a different sensor (described in Section 2.2) with different backgrounds from two distinct cotton varieties (FM2011 and FM2484) over a different time period (2019 growing season), and at a different location as compared to sites I and II. Overall, this study used UAV measurements from three cotton varieties, two tillage practices, seven cover crop treatments, six different irrigation conditions, two different irrigation regimes (irrigated and rainfed), and two different years.

#### 2.2. Data collection

#### 2.2.1. UAV measurements and preprocessing

At experiment site III, a Phantom 4 Pro (P4P; DJI, China) quadcopter equipped with a DJI FC6310 RGB (red, green, blue) (DJI, China) optical sensor (Fig. 1a) was used during the 2019 growing season. To collect UAV measurements from experiment sites I and II during the 2021 season, a Matrice 200 (M200; DJI, China) quadcopter equipped with a MicaSense Rededge multispectral (AgEagle Aerial Systems Inc, USA) optical sensor (Fig. 1b and 1c) was used. All of the flights were performed within one hour of solar noon, with little to no cloud cover and winds less than 15 km/h. The Pix4Dcapture mobile app, developed by Pix4D S.A., Switzerland, was used to create the flight plans with the flight characteristics shown in Table 1. The flight altitude was set in order to obtain images with a spatial resolution close to 1 cm. Eighty-five percent front and side overlaps were employed to target oversampling and compensate for errors introduced by the uncalibrated/blurred/

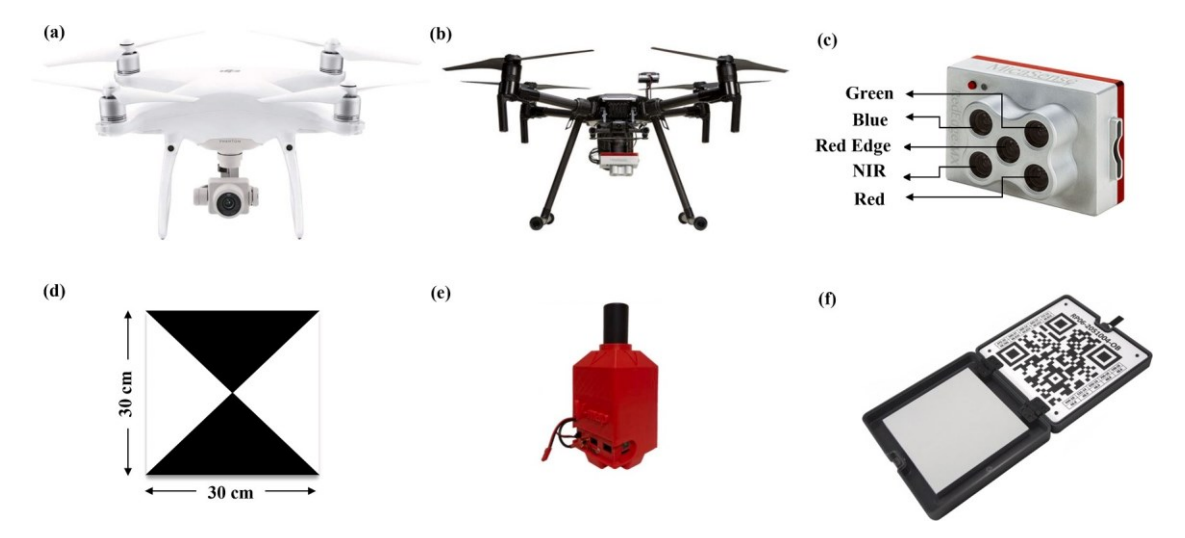


Fig. 1. Unmanned Aerial Vehicle (UAV) imaging platforms and other instruments: (a) DJI Phantom 4 pro quadcopter equipped with DJI FC6310 RGB sensor, (b) Matrice 200 quadcopter equipped with MicaSense Rededge multispectral sensor, (c) MicaSense Rededge multispectral camera, (d) ground control point unit, (e) V-map dual-frequency global navigation satellite system, (f) MicaSense calibrated reflectance panel.

Table 1
Characteristics of UAV flights and measurements.

| UAV measurements         |                  |                   |  |  |  |
|--------------------------|------------------|-------------------|--|--|--|
| Year                     | 2019             | 2021              |  |  |  |
| Date                     | October 21, 2019 | October 31, 2021  |  |  |  |
| Drone                    | Phantom 4 Pro    | Matrice 200       |  |  |  |
| Sensor                   | DJI FC6310       | MicaSense Rededge |  |  |  |
| Bands                    | RGB              | RGB, RE, NIR      |  |  |  |
| Bands used in boll count | RGB              | RGB               |  |  |  |
| Front overlap            | 85%              | 85%               |  |  |  |
| Side overlap             | 85%              | 85%               |  |  |  |
| Height                   | 30 m             | 15 m              |  |  |  |
| GCPs                     | 8                | 8                 |  |  |  |
| Georeferencing RMSE      | 1.1 cm           | 1.4 cm            |  |  |  |
| Spatial resolution       | 0.75 cm          | 1.07 cm           |  |  |  |
| Experiment site          | III              | I and II          |  |  |  |

Note: R- Red; G- Green; B- Blue; RE- Red Edge; NIR- Near-Infrared; GCP- Ground Control Point; RMSE: Root Mean Square Error.

#### geometrically distorted images [1].

All captured images were geotagged in real-time using the onboard GPS systems installed in the quadcopter platforms. In addition, eight ground control points (GCPs; Fig. 1d) were employed in the field to generate georeferenced data products with high precision. The coordinates of the GCPs were measured using the V-map dual frequencypost processed static (PPS) global navigation satellite system (GNSS; Fig. 1e; Micro Aerial Projects, USA) and they were used to georeference the orthomosaic images. As recommended by Rouze et al. [18], orthomosaic images with less than 1.5 times the pixel resolution georeferencing root mean square error (RMSE) were extracted in GeoTiff format for further image processing. Additionally, a MicaSense calibrated reflectance panel (Fig. 1f) supplied by MicaSense was used to radiometrically calibrate the captured images in order to perform an illumination adjustment and obtain more accurate reflectance values. During this calibration process, one image per band of the calibration panel was captured at the time of flight and the spectral reflectance of the processed images was adjusted based on the fixed reflectance values of the panel. More details about the calibration panel and spectral reflectance correction can be found at MicaSense knowledge base (https://support. micasense.com/).

#### 2.2.2. Manual data collection for cotton boll count and cotton yield

Ground truth data for cotton boll count and yield were collected from the experimental sites to validate the algorithm developed for counting cotton bolls. Cotton bolls were counted using a 1 m X 1 m area in two middle rows (rows 4 and 5) per plot at sites I and II and from a set of five plants in one row per cotton cultivar per plot at the third experiment site. The coordinates of the ground truth data location area were recorded using V-map PPS GNSS. These locations were also marked with flags so that the same plants were monitored throughout the growing season and also to easily detect ground truth data locations in the UAV images and minimize errors associated with GPS instruments. Ground truth data for cotton boll count was collected one week before harvesting from 12 to 21 plots at experiment sites I and II, respectively, in 2021 and from 48 plots at experiment site III in 2019. Whereas ground truth data for cotton yield was collected from 12 to 21 plots at experiment sites I and II, respectively, in 2021 and from 128 plots at experiment site III in 2019. This ground truth information on cotton yield was used for developing a relation between cotton boll count and cotton yield in this study.

#### 2.3. Image processing

The methodology proposed for cotton boll counting (Fig. 2) consists of two parts. First, the collected images were subjected to an image processing pipeline for the cotton boll candidate recognition. The goal of the cotton boll candidate recognition was to segment cotton boll pixels from the surrounding background, which included soil, weed, foliage/residuals, leaves, and branches. To remove non-cotton boll pixels, a python programming-based pipeline was developed, as described in Section 2.3.1. The output from this step was a binary image in which cotton boll candidate pixels were classified with pixel intensities of one and the non-cotton-boll pixels with pixel intensities of zero. This binary image was further converted into a polygon vector of cotton boll candidates.

In the second stage, an ML-based SVR model was adopted to count the total number of bolls in each segmented cotton boll candidate identified in the previous step. The response variable in this SVR model was the number of cotton bolls in a cotton boll candidate with four predictors comprising geometric aspects of the cotton boll candidate, including area, perimeter, maximum length, and roundness. The final outcome of this process was a polygon vector of cotton boll candidates with information on the number of cotton bolls in each candidate.

#### 2.3.1. Cotton boll candidate recognition

The cotton boll candidate recognition was performed in four stages using a band-mean filter, the Otsu thresholding [16], a red/blue band

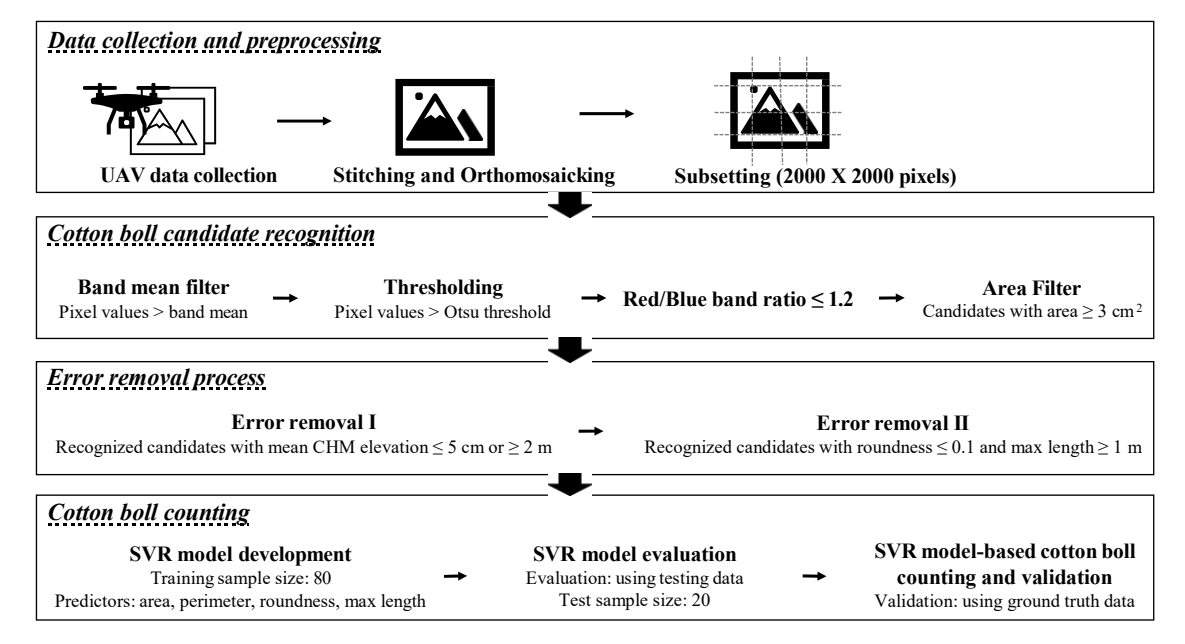


Fig. 2. Flowchart of the processes involved in the proposed approach for counting cotton bolls. (Note: UAV- Unmanned Aerial Vehicle, SVR- Support Vector Regression).

ratio filter, and an area filter. The primary goal of this candidate selection approach was to eliminate the background pixels of the image, including plant shadows, foliage/residue, dark ground, and weeds. The spectral behaviors of these classes across the RGB bands were analyzed at all three sites (Fig. 3) by averaging the pixel values of 20 randomly selected samples within each class, with a minimum of 10 pixels per sample. Cotton boll pixels were found to be associated with the highest reflectance. Therefore, in the first stage, a band-mean filter was applied to remove dark pixels. In this process, the pixels having a lower reflectance value than the mean value of each band in all three RGB bands were filtered out (Fig. 4b and 4d). A majority of the remaining pixels after the band-mean filtering process belonged to cotton boll and soil classes.

One of the most challenging tasks in image processing is to separate pixels with identical reflectance values using a threshold. Selecting a fixed threshold to separate these remaining two major classes from different UAV images could lead to error due to varying spectral properties of the images depending upon UAV sensors, field conditions, and several other environmental and instrumental factors. The Otsu method was employed in this study to set an independent threshold for each scene using the spectral properties of the filtered pixels. The Otsu method is an automatic thresholding approach that determines the

threshold by minimizing intra-class variation and maximizing inter-class variation [16]. A bimodal distribution was discovered in the reflectance histogram of filtered pixels in the R, G, and B channels suggesting the presence of two major classes i.e., soil/bright weed and cotton boll. The Otsu thresholding approach divided the filtered pixels into two classes: (i) low reflectance class, which represented bright weed and bare soil pixels, and (ii) high reflectance cotton boll candidate pixels (Fig. 4e). All low reflectance pixels were then masked out, thereby eliminating a majority of the background pixels (Fig. 4c). To ensure the complete removal of all background pixels, a third filter, red/blue band ratio, was used. This filter was used to further eliminate the non-target pixels. It was observed from the spectral signature analysis (Fig. 3) that cotton boll pixels showed similar digital number values on all three bands indicating a red/blue band ratio close to one. Therefore, pixels with a red/blue band ratio greater than 1.2 were thus filtered out. Additionally, an area filter was applied to remove noise from the data assuming that a single cotton boll would have a minimum of 3 cm<sup>2</sup> area.

# 2.3.2. Errors associated with recognition of cotton boll candidates and their removal

Following the cotton boll candidate recognition process, a preliminary inspection of output binary images revealed few challenges or

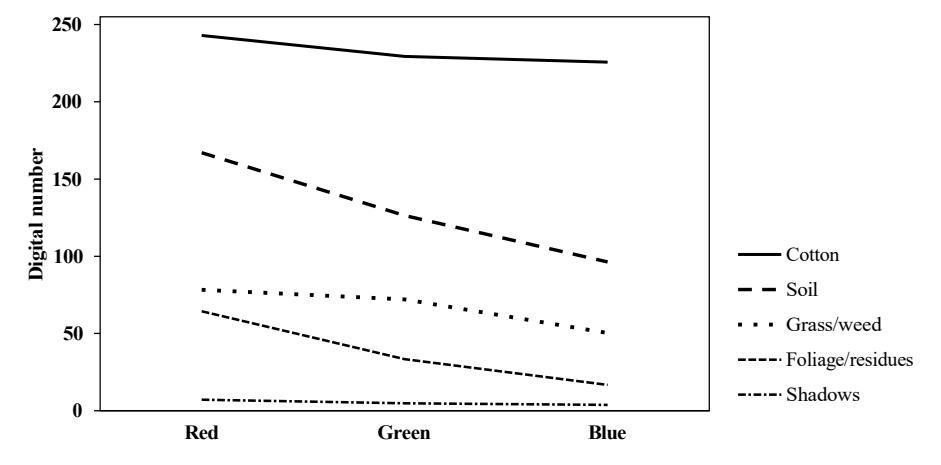


Fig. 3. Spectral signatures of different classes across red, green, and blue bands.

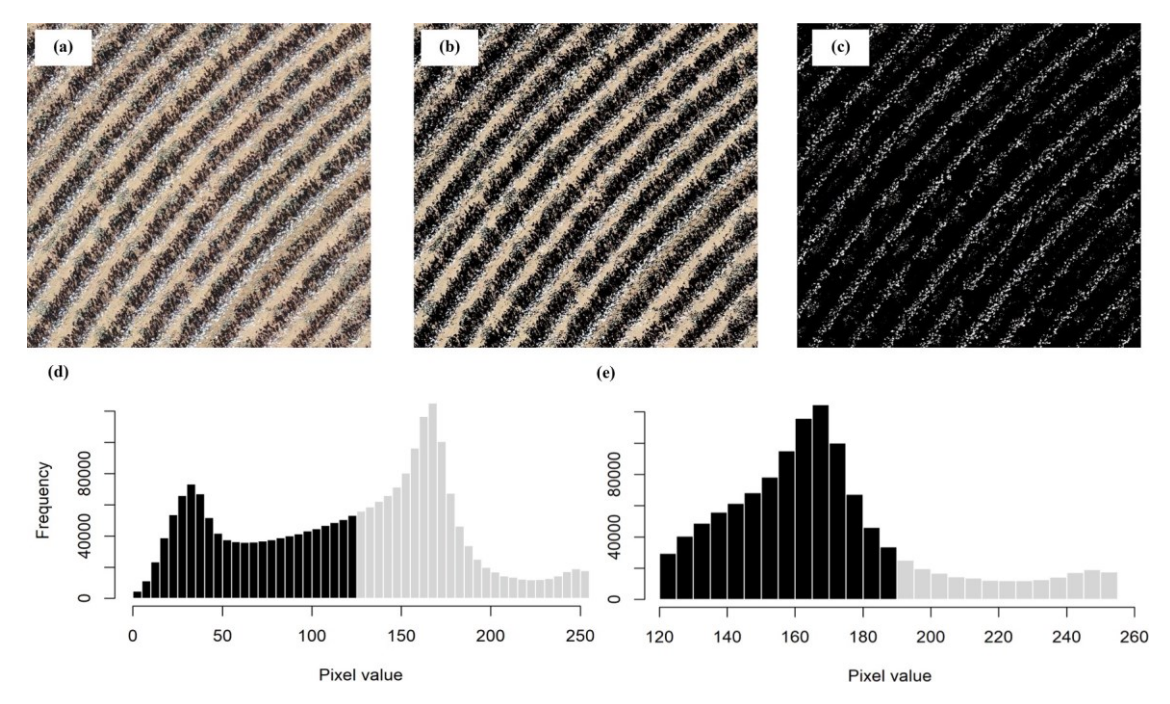


Fig. 4. Cotton boll candidate recognition process outputs: (a) subset of orthomosaic image from experiment site III, (b) image after applying band-mean filter, (c) image after applying Otsu threshold, (d) histogram of pixel values for blue band in the orthomosaic image; black columns representing pixel values less than the band mean, (e) histogram of pixel values for blue band after the band-mean filtration process; black columns representing pixel values less than the Otsu threshold.

potential error sources that could introduce substantial errors in boll count and yield predictions. In this study, three error sources were recognized, including bright weed (Fig. 5a), center pivot system parts (Fig. 5b), and cotton bolls on the ground (Fig. 5c) pixels, which were misclassified as cotton boll candidates. These error pixels had similar spectral properties as those of cotton boll pixels, and thus they could not be removed using previously applied spectral filters. Consequently, two additional steps (Fig. 2) were adopted to exclude these misclassified pixels. First, an elevation filter was implemented to remove error pixels associated with cotton bolls on the ground and parts of the center pivot system since they were at different elevations as compared to the cotton bolls on the plants. A canopy height model (CHM), resampled to the spatial resolution of the orthomosaic image, was developed using digital surface and terrain models. Details about the CHM generation process using UAV imagery can be found in Chang et al. [3]. The recognized candidates that are either less than 5 cm or greater than 2 m elevation in CHM were removed. Some parts of the center pivot system were, however, present in between the selected threshold elevation criteria and they were therefore still misclassified as cotton boll candidates. A filter with a combination of roundness index (< 0.1) and maximum length (>1 m) was implemented to filter these misclassified candidates. Here, the maximum length of the candidates was defined as the maximum length among all the combinations of vertex-to-vertex lengths of the candidate and the roundness was calculated using Eq. (1) [27]:

$$Roundness = \frac{4\pi * Area}{Perimeter^2}$$
 (1)

#### 2.3.3. Boll counting

Varying sizes and complex shapes of cotton bolls pose challenges in counting the number of bolls in a cluster of cotton bolls. In addition, the orientation and overlapping of cotton bolls make cotton boll counting from UAV images even more challenging. Clusters composed of several overlapping cotton bolls generally have a larger area and elongation ratio than a single cotton boll. However, these clusters may have a similar elongation ratio as that of a single cotton boll. In addition, a single cotton boll can have a round or non-round/elongated structure, depending upon the boll facing angle when detected by the UAV sensors.

As a result, counting the number of cotton bolls from a cotton boll candidate using a simple threshold for area or elongation ratio or using a combination of these thresholds can lead to errors. Therefore, we implemented an SVR-based ML approach to overcome these limitations and account for all complex and varied sizes of cotton bolls in the images. The SVR is a regression version of the SVM that is used to develop the relation between a dependent variable and one or more independent variables. A detailed description of the SVR can be found in Smola and Schoʻlkopf [21] and Tian et al. [24].

In this study, the approach proposed for cotton boll counting from segmented candidates includes a supervised SVR model with four geometric aspects of the cotton boll candidates as feature vectors: area, parameter, roundness, and maximum length. These feature vectors and their corresponding labels were used to train a non-linear kernel function based SVR model. Before training SVR model in R, a trainControl (Package: caret) function was used to generate parameters that control computational nuances of the train (Package: caret) method. The repeatedCV (repeated cross-validation) resampling method with three separate 10-fold cross-validation was used as resampling scheme for the trainControl function. The SVR model was trained using train function with the svmRadial method. The train function fits predictive models over different tuning parameters, evaluates the effect of tuning parameters on model performance, and selects an optimal model across the tuning parameters considered. A preprocessing of the training data using the "center" & "scale" parameters in the train function was also incorporated to standardize training data. The train function selected the optimal SVR model for the training data at C = 2 (penalty parameter of the error term) using the smallest RMSE values at different C values.

The SVR model was trained using 80 training samples and evaluated over 20 test samples. The training and test samples for the SVR model were collected through visual inspection from the orthomosaic images of experiment site II. The samples were chosen in such a way that a wide variation in candidate area was captured. Further, the *createDataPartition (Package: caret)* function was used to create stratified random samples based on cotton boll count (i.e., response variable) and split the samples into training and test data. Three independent users counted the number of cotton bolls in the selected sample candidates

# Before error removal After error removal a) Bright weed pixels b) Pivot pixels c) Cotton on ground and other white pixels

Fig. 5. Snapshots of orthomosaiced UAV image from experiment site III with recognized cotton boll candidate polygons before (red) and after (blue) the error removal process. (Note: Green arrow is pointing to the falsely classified pixel of cotton on ground before and after the error removal process).

using visual inspection of the ortho-mosaiced images, and the mean values from the three inspections were recorded as a response variable in the SVR model. The evaluated SVR model was then used to count the number of cotton bolls in the segmented candidates across all three experiment sites.

#### 2.4. Statistical analysis

The accuracy of the candidate recognition process, before and after the removal of error sources, was assessed using visual inspection of 1000 randomly selected pixels (500 cotton boll candidates and 500 background pixels) for each experiment site. The confusion matrix and precision-recall methods were implemented to evaluate the quality of the output of the candidate recognition process by classifying the data into four categories, namely, true positive (TP), true negative (TN), false positive (FP), and false negative (FN). The TP and TN categories represented the correctly recognized pixels whereas FN and FP represented the omission and commission errors, respectively. The accuracy of the candidate recognition process was further assessed using three statistical metrics presented in Eqs. (2)–(4):

$$Classification\ accuracy = \frac{TP + TN}{total\ number\ of\ pixels} \tag{2}$$

$$Precision = \frac{TP}{TP + FP} \tag{3}$$

$$Recall = \frac{TP}{TP + FN} \tag{4}$$

While classification accuracy represents the fraction of correctly classified pixels among all pixels, precision represents the fraction of retrieved pixels that were relevant to the query, and recall represents the fraction of relevant pixels that were successfully retrieved.

The proposed SVR-based cotton boll counting approach was quantitatively validated using a two-step approach. First, the performance of the established SVR model was evaluated for training and test data. Later, the estimated number of cotton bolls was compared with the measured/ground truth cotton boll count data for validation. Three statistical metrics, viz., coefficient of determination (R<sup>2</sup>), mean absolute percentage error (MAPE), and root mean square error (RMSE) were used to evaluate the performance of the SVR-based cotton boll counting

approach Eqs. (5)–((7)).

$$R^{2} = \sum_{i=0}^{\infty} \frac{[\mathbf{\Sigma}(P_{i} - \overline{P})(O_{i} - \overline{O})]^{2}}{(P_{i} - \overline{P})^{2} * \mathbf{\Sigma}(O_{i} - \overline{O})^{2}}$$
(5)

$$MAPE = \frac{100}{n} \sum_{i=1}^{n} \frac{O_i - P_i}{O_i}$$
 (6)

$$RMSE = \frac{1}{n} \underbrace{0}_{i=1}^{n} P(C_{i} - P)$$
 (7)

where, n is the number of plots, and  $O_i$  and  $P_i$  are the observed (or ground truth) and predicted number of cotton bolls. Additionally, observed and predicted boll count data were plotted and compared for the agreement with the 1:1 line.

#### 2.5. Lint yield prediction and validation

The number of cotton bolls estimated from the UAV images is typically lower than the actual number of bolls due to the covering of lower canopy cotton bolls by upper canopy cotton bolls while collecting UAV images with the sensor pointed to the nadir direction. However, we found a high correlation between the UAV detected boll count and

actual boll count in this study with a low MAPE (discussed in Section 3.1.2). Therefore, we used a linear regression analysis to develop relations between lint yield and UAV estimated boll count and candidate area. Lint yield prediction relations were developed for each variety, assuming that the weight of each variety's cotton boll is different. A

multiple linear regression approach was also used while considering both boll count and candidate area as predictors. These yield prediction relations were developed using 75% of observed lint yield data as training data and the remaining 25% of the data as the testing data for each cotton variety. The createDataPartition (Package: caret) function was used to split the data into training and test data, and to create a stratified random sample considering observed yield data as response variable. The developed linear relations were compared and evaluated using four statistical metrics: R2, RMSE, MAPE, and Nash-Sutcliffe Efficiency (NSE; Eq. (8)).

NSE = 1 - 
$$\sum_{i=1}^{n} (P_i - O_i)^2 \atop \sum_{i=1}^{n} (O_i - O)^2$$
 (8)

#### a.) Before error sources removal

|         | Predicted Class |                      |                      |  |  |
|---------|-----------------|----------------------|----------------------|--|--|
|         |                 | Positive             | Negative             |  |  |
| ılClass | Positive        | 481<br>True Positive | 19<br>False Negative |  |  |
| Actual  | Negative        | 31<br>False Positive | 469<br>True Negative |  |  |

|      |       | Predicted | l Class |
|------|-------|-----------|---------|
|      |       | Positive  | Nega    |
| lass | itive | 492       | 8       |

|         |          | Positive             | Negative             |
|---------|----------|----------------------|----------------------|
| alClass | Positive | 492<br>True Positive | 8<br>False Negative  |
| Actu    | Negative | 29<br>False Positive | 471<br>True Negative |

| Ш    |
|------|
| ite  |
| tS   |
| ıen  |
| riii |
| kpe  |
| -3   |

Experiment Site II

|              | Predicted Class |                      |                      |  |  |
|--------------|-----------------|----------------------|----------------------|--|--|
|              |                 | Positive             | Negative             |  |  |
| Actual Class | Positive        | 464<br>True Positive | 36<br>False Negative |  |  |
| Actu         | Negative        | 74<br>False Positive | 426<br>True Negative |  |  |

#### b.) After error sources removal

|              | Predicted Class  |                      |                      |  |  |  |
|--------------|--|----------------------|----------------------|--|--|--|
|              |  | Positive             | Negative             |  |  |  |
| Actual Class | Positive Pos | 481<br>True Positive | 19<br>False Negative |  |  |  |
| Actu         | Negative   | 13<br>False Positive | 487<br>True Negative |  |  |  |

|              | Predicted Class |                      |                      |  |  |  |
|--------------|-----------------|----------------------|----------------------|--|--|--|
|              |                 | Positive             | Negative             |  |  |  |
| Actual Class | Positive        | 492<br>True Positive | 8<br>False Negative  |  |  |  |
| Actu         | Negative        | 10<br>False Positive | 490<br>True Negative |  |  |  |

|              | Predicted Class            |                      |                      |  |  |
|--------------|----------------------------|----------------------|----------------------|--|--|
| Positive     |                            | Positive             | Negative             |  |  |
| Actual Class | Dositive 464 True Positive | 36<br>False Negative |                      |  |  |
| Actu         | Negative                   | 21<br>False Positive | 479<br>True Negative |  |  |

Fig. 6. Experiment-wise confusion matrix for accuracy assessment of cotton boll candidate recognition process.

#### 3. Results

#### 3.1. Validation of cotton boll counting approach

#### 3.1.1. Accuracy assessment of cotton boll candidate recognition process

Fig. 6 and Table 2 show the confusion matrix and values of statistical metrics related to evaluation of the candidate recognition process. Although the evaluation statistics suggested high classification accuracy in extracting cotton boll candidates even before removing the errors, output images still contained falsely classified pixels. The greatest error was noted for the experiment site III, which was primarily due to the presence of a large number of bright weed and pivot part pixels (Fig. 5). The bright soil pixels introduced additional commission errors (mistakenly accepting a false observation) in the candidate recognition process for the experiment site III. The commission errors at experiment sites I and II (Fig. 6) were only due to bright soil pixels.

The digital numbers for these error pixels were found to be comparable to those of cotton boll pixels in all three bands, implying that these pixels could not be segmented from the cotton boll pixels solely based on spectral properties. Therefore, mean elevation, max length, and roundness parameters of recognized candidates were used in the error removal process. This approach improved the accuracy of candidate extraction process (Table 2) by removing commission error pixels while it did not affect omission error (mistakenly rejecting a true observation; Fig. 7) pixels. High values for precision and recall after the error removal process indicated a low number of falsely identified pixels among the recognized pixels and identification of a high proportion of true cotton boll pixels, respectively. Overall, the observed statistical metrics indicated that the cotton boll candidate recognition technique was highly effective in segmenting cotton bolls and background pixels (Fig. 8).

#### 3.1.2. SVR-based cotton boll counting approach

The SVR model performance in estimating the total number of cotton bolls was good as indicated by only 0.55% error during training and 3.6% error during validation (Table 3). The evaluated model was then used to estimate boll count from the image of the entire experimental area at each site. Fig. 8 depicts the outcomes of the candidate recognition and cotton boll counting steps for a single cotton plant. The estimated boll count was then validated against the observed/ground truth boll count. Fig. 9 and Table 4 show the correlation analysis between the estimated and observed boll counts. The high correlation and associated low MAPE values found for all three sites (Fig. 9) suggested a good agreement between the observed and estimated boll counts. Overall, the evaluation and validation statistics suggested that the use of geometric features of segmented candidates as predictors in association with the SVR model demonstrated a good performance in estimating boll count from recognized cotton boll candidates.

#### 3.2. Lint yield prediction

Cotton boll count and candidate area were found to be highly correlated with lint yield in the linear regression analysis (Fig. 10). Multiple linear regression was used to test if both parameters, i.e., cotton boll count and candidate area predicted lint yield well. Fig. 10 shows the fitted regression models, and Table 5 presents the information on statistical metrics and fitted model equations for all three cotton cultivars

Table 2

Experiment-wise statistical metrics for accuracy assessment of cotton boll candidate recognition process (before and after error removal).

| Statistical metrics     | Site I |       | Site II |       | Site III |       |
|-------------------------|--------|-------|---------|-------|----------|-------|
|                         | Before | After | Before  | After | Before   | After |
| Classification accuracy | 0.95   | 0.97  | 0.96    | 0.98  | 0.89     | 0.94  |
| Precision               | 0.94   | 0.97  | 0.94    | 0.98  | 0.86     | 0.96  |
| Recall                  | 0.96   | 0.96  | 0.98    | 0.98  | 0.93     | 0.93  |



Fig. 7. Omission error resulting from pivot shadowed pixels at experiment site III.

Table 3
Evaluation statistics of developed SVR model for the training and test datasets.

| Parameters                                 | Training | Test |
|--|----------|------|
| Total predicted cotton bolls               | 362      | 81   |
| Total original cotton bolls                | 364      | 84   |
| Difference                                 | 2        | 3    |
| Percent Error                              | 0.5      | 3.6  |
| Misclassification error from the model (%) | 5        | 25   |

used in the field experiments. It was found that the candidate area did not contribute significantly (p>0.05) to lint yield prediction under multiple linear regression models. However, in the fitted linear regression models, candidate area showed high correlation with lint yield  $(R^2=0.55-0.85;$  Table 5) for all cotton cultivars and significantly predicted lint yield (p<0.05). Overall, the statistical metrics indicated the boll count as a better predictor of lint yield than the candidate area, with higher  $R^2$  and NSE values and lower RMSE and MAPE values (Table 5). Although multiple linear regression models predicted lint yield better, the yield prediction did not improve much in comparison to the linear regression model using boll count alone as a predictor (Table 5).

#### 4. Discussion

In this study, a simplified cotton boll candidate recognition algorithm was developed using simple spectral filters and an SVR-based machine learning tool. The evaluation and validation statistics suggested that this method can reliably recognize and estimate cotton boll count from RGB-based UAV measurements collected after defoliation at the late boll opening cotton growth stage. The UAV imagery collected after defoliation resulted in a relatively simple background with few to no green leaves covering or casting shadows on the cotton bolls in the lower canopy. Additionally, UAV flights during solar noon produced images free from shadows and minimized the omission errors. An 85% front and side overlap was set while taking UAV measurements to target oversampling, which helped in avoiding image gaps introduced during the orthomosaicking process when removing uncalibrated/blurred/ geometrically distorted images [1]. In addition, taking UAV measurements at solar noon with a wind speed of less than 15 kmph resulted in low commission errors. Therefore, this study recommends collecting and processing UAV measurements in the above-mentioned manner as the first step to minimize error sources and obtain high accuracy with the proposed candidate recognition process.

Although the errors in candidate recognition were small, these error pixels could introduce significant errors in cotton yield estimates if yield estimates are solely based on the area under the recognized candidates [27] or boll count [18]. Therefore, we included an error removal step to remove major commission error pixels and improve the performance of

Fig. 8. Cotton boll count pipeline: (a) UAV captured orthomosaic image, (b) cotton boll candidate recognition using spectral properties, and (c) cotton boll count using geometrical features of recognized candidates.

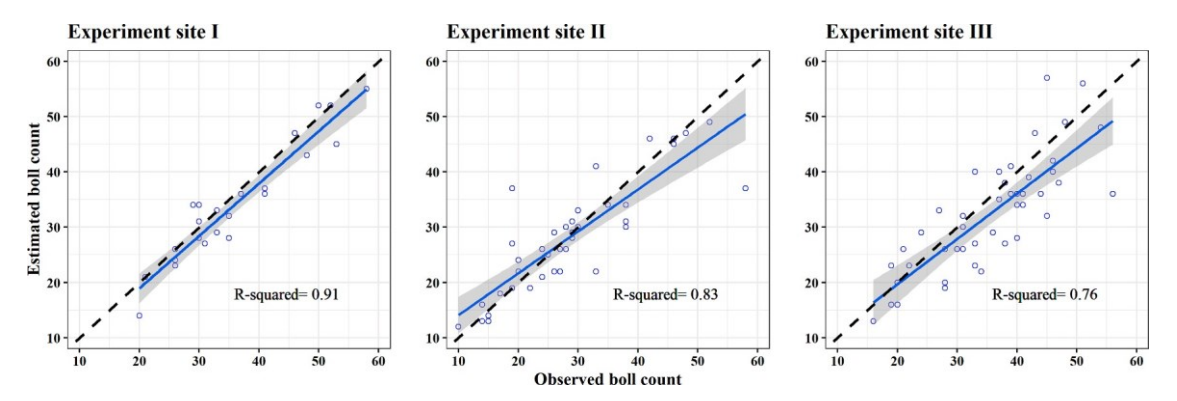


Fig. 9. Experiment-wise correlation analysis of estimated and ground-truth observations for cotton boll count [Note: Dotted black line - 1:1 line; Blue line - Line of best fit].

Table 4
Experiment-wise statistical metrics for correlation analysis of estimated and ground-truth observations for cotton boll count.

| Experiment site | Statistical Metrics |       |        |  |
|-----------------|---------------------|-------|--------|--|
|                 | R <sup>2</sup>      | RMSE  | MAPE   |  |
| Site I          | 0.91                | 4.14% | 5.80%  |  |
| Site II         | 0.83                | 5.80% | 0.69%  |  |
| Site III        | 0.76                | 7.07% | 11.46% |  |

Note: R<sup>2</sup>: Coefficient of determination; RMSE: Root mean square error; MAPE: Mean absolute percentage error.

the candidate recognition process. Different types of error sources in the UAV images from different sites, particularly error sources with similar spectral properties to cotton bolls in RGB bands, suggested a need for the consideration of non-spectral filters to minimize with these errors. After a preliminary evaluation of the outputs of the candidate recognition process and identification of the error sources, this study considered mean CHM, roundness, and the maximum length of recognized candidates as non-spectral filters because error sources were found to be elongated and at a different height as compared to the target cotton boll pixels.

In this study, band-mean digital number values ranged from 121 to 147 and the Otsu threshold ranged between 163 and 186 for the blue band. The observed long range of band-mean and Otsu thresholding indicated the importance of selecting thresholds based on the spectral properties of the image or a subset of the image. Selecting a fixed threshold could lead to a high omission or commission error due to removal of lower reflectance cotton boll pixels or inclusion of higher reflectance background pixels, respectively. For example, Jung et al. [11] used a threshold value of 190 for the red band to segment cotton boll pixels from the background, which worked well for that study area,

but using this threshold for UAV images in this study led to high omission error. We also used a fixed red/blue band ratio of 1.2 in the candidate recognition process to avoid high omission error, but we recommend evaluating classification accuracy by changing this threshold value. However, given the high classification accuracy obtained for complex backgrounds across seven different cover crop treatments in this study, a fixed threshold of 1.2 for the red/blue band ratio can provide satisfactory results. In this study, cotton boll pixels in the lower canopy were primarily responsible for the omission errors. These pixels were shadowed by the upper canopy, resulting in lower digital numbers, and they were eliminated during the background filtration processes. This study did not include steps for removal of omission error sources due to high complexity of removal process and presence of low omission error values

The SVR algorithm is generally considered as a relatively simple method in ML, however robust in its performance, because the final decision function is determined by only a few support vectors [15]. Here, support vectors are nonlinear combinations derived from geometric aspects of the cotton boll candidate, namely area, perimeter, max length, and roundness. In this study, the SVR-based cotton boll count approach showed potential to extract information from complex shapes of clusters. However, this approach might not estimate the exact number of cotton bolls in a large cluster due to large overlapping and different orientations of cotton bolls. These large clusters were the key source of classification error for the test data. However, our approach performed very well for the small clusters of less than six cotton bolls. A larger training dataset with a greater number of large clusters could be useful to further improve this approach to reduce classification errors. Nonetheless, the small error found in the overall boll count during both training and testing demonstrated the applicability of this boll count algorithm. The identification of true boundaries of the individual cotton bolls within a cluster was not considered in this study since it could

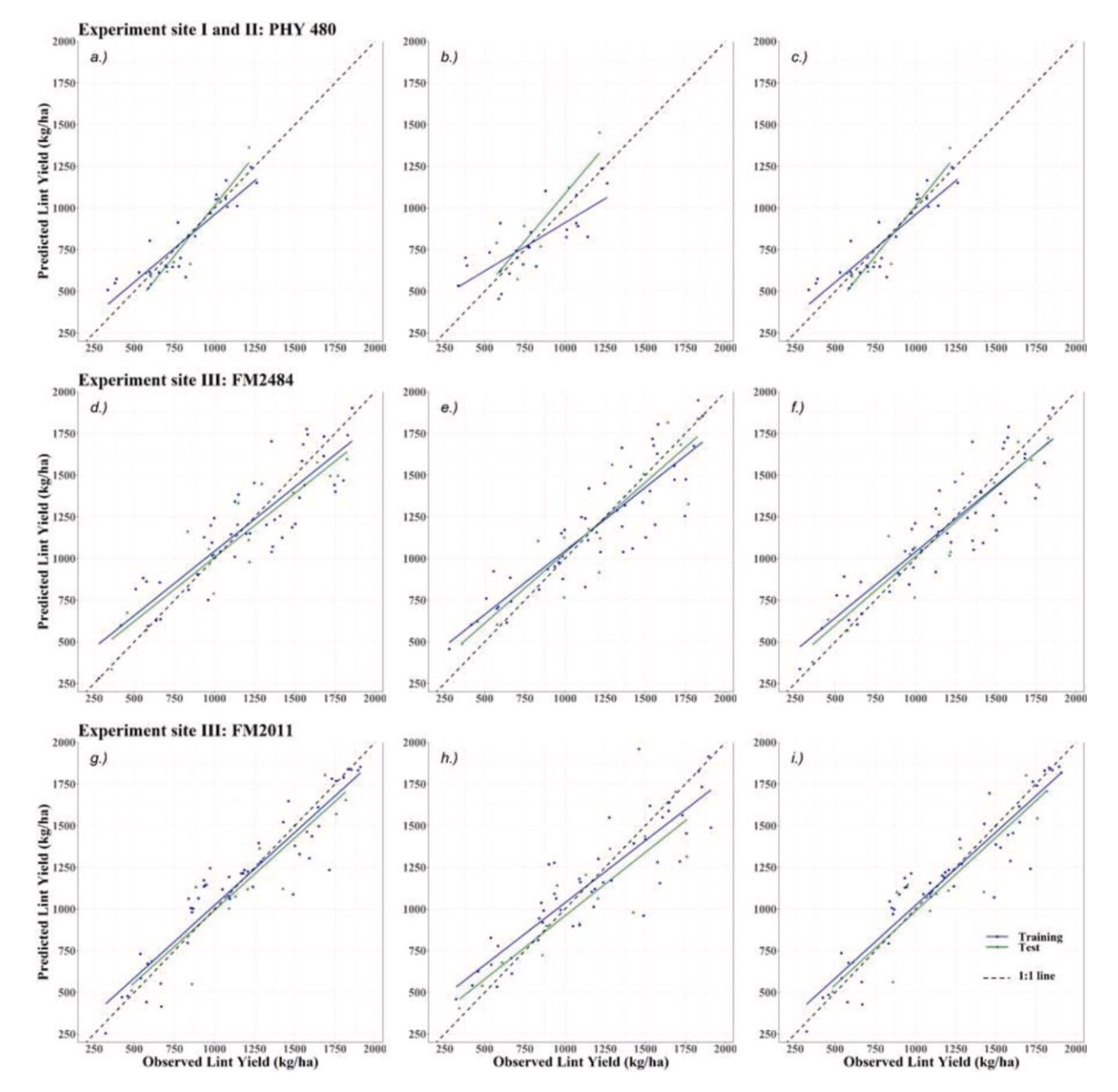


Fig. 10. Variety-wise cotton yield prediction using cotton boll count (left column: parts a, d, and g), recognized candidate area (middle column: parts b, e, and h); and cotton boll count and candidate area (right column: parts c, f, and i) as predictors.

result in loss of cotton boll pixels and reducing the area under recognized candidates, which is a potential predictor of cotton yield. The linear regression analysis for predicting lint yield using boll count and candidate area suggested that lint yield was sensitive to both predictors, but boll count had a greater impact on lint yield than the candidate area. While the proposed boll count approach addressed some of the issues related to overlapping and clustering, it did not change the area under the recognized cotton boll candidates.

In this study, the UAV imageries taken at the nadir (pitch = 90°) direction were used to validate the proposed approaches. However, some cotton bolls were present in the lower canopy and some other bolls had a downfaced orientation. Although these conditions were limited, they resulted in a slight underprediction of boll count since these bolls were not visible in the captured images. Future studies can explore the suitability of different pitch angles for UAV sensors for estimating cotton boll count. Although the methods proposed in this study showed high

accuracy, there is still scope to improve the cotton boll recognition and counting processes. For, example, this study utilized a common red/blue band ratio threshold of 1.2 which can be changed as per the UAV measurements and background characteristics. Another improvement can be through the increase of training sample size or increasing the number of predictors in the model development to increase the accuracy of the SVR model. Utilizing more complex approaches such as artificial or convolutional neural network-based deep learning approaches could also improve the boll counting process. Generating 3-D data such as using LiDAR could also be effectively implemented for the error removal steps in the proposed cotton boll count approach as well as to quantify the spatial distribution of bolls [23]; however, that would increase the cost and complexity of the process. Another limitation of this study is that it considered only three cotton cultivars. Cotton varieties affect spatial distribution and the number of cotton bolls in the lower canopy, and hence affect the omission error in the UAV measurements.

 Table 5

 Variety-wise regression models for cotton yield prediction.

| Cotton Cultivar   | Training       |      |        |      | Test           |      |        |      |  |                   |                |
|---|----------------|------|--------|------|----------------|------|--------|------|--|-------------------|----------------|
|   | $\mathbb{R}^2$ | NSE  | RMSE   | MAPE | $\mathbb{R}^2$ | NSE  | RMSE   | MAPE | Model                                    | p-value           |                |
| Linear Regression- Boll Count                             |                |      |        |      |                |      |        |      |  |                   |                |
| PHY480  | 0.81           | 0.81 | 112.83 | 0    | 0.90           | 0.79 | 94.65  | -2.3 | Y = 0.0018*X + 349.63                    | < 0.001           |                |
| FM2484  | 0.77           | 0.77 | 195.23 | 0    | 0.85           | 0.83 | 181.07 | -2.6 | Y = 0.0026 * X - 183.42                  | < 0.001           |                |
| FM2011  | 0.87           | 0.87 | 157.56 | 0    | 0.87           | 0.85 | 188.53 | -5.4 | Y = 0.0035*X - 241.07                    | < 0.001           |                |
| Linear Regression - Candidate Area                        |                |      |        |      |                |      |        |      |  |                   |                |
| PHY480  | 0.58           | 0.58 | 168.05 | 0    | 0.79           | 0.55 | 140.31 | 7.5  | Y = 1.37*X + 290.87                      | < 0.001           |                |
| FM2484  | 0.76           | 0.76 | 199.05 | 0    | 0.82           | 0.81 | 191.64 | 0.8  | Y = 1.26*X + 250.42                      | < 0.001           |                |
| FM2011  | 0.77           | 0.77 | 211.83 | 0    | 0.85           | 0.84 | 190.98 | -4.1 | Y = 1.67*X + 240.74                      | < 0.001           |                |
| Multiple Linear Regression- Boll count and Candidate Area |                |      |        |      |                |      |        |      |  | <b>Boll Count</b> | Candidate Area |
| PHY480  | 0.81           | 0.81 | 112.83 | 0    | 0.9            | 0.79 | 94.31  | -2.4 | $Y = 0.0019 * X_1 - 0.01 * X_2 + 351.36$ | < 0.001           | NS             |
| FM2484  | 0.79           | 0.79 | 186.65 | 0    | 0.86           | 0.85 | 170.32 | -1.1 | $Y = 0.0015*X_1 + 0.59*X_2 - 22.69$      | NS                | NS             |
| FM2011  | 0.88           | 0.88 | 156.40 | 0    | 0.88           | 0.86 | 180.84 | -5.4 | $Y = 0.0031 * X_1 + 0.21 * X_2 - 204.01$ | < 0.001           | NS             |

Note: R<sup>2</sup>: Coefficient of determination; NSE: Nash-Sutcliffe model efficiency coefficient; RMSE: Root mean square error; MAPE: Mean absolute percentage error; X<sub>1</sub>: Boll count: X<sub>2</sub>: Candidate area.

Therefore, there is a need for an omission error removal process under certain cotton varieties.

#### 5. Conclusion

This study proposed a simplified cotton boll candidate recognition process, followed by a cotton boll count method within the recognized candidates. The evaluation statistics of the candidate recognition process indicated that the spectral properties of the cotton and background pixels could be effectively used to segment cotton boll pixels from the UAV images. The classification accuracy assessment of the candidate recognition process revealed that there could be background/nontarget pixels that introduce commission errors (false positives) due to similar spectral properties to cotton boll pixels in UAV images, such as bright soil or weed pixels, that cannot be segmented using spectral filters. The commission error removal processes implemented in this study highlighted the utilization of the CHM and geometrical features of recognized candidates to improve classification accuracy. The shadowed cotton boll pixels were found to be the source of omission error (false negative). This study did not include the omission error removal steps due to presence of low omission errors and to avoid computational complexity.

The boll count method also performed promisingly, with a slight underestimation of the number of cotton bolls. A potential source for the underestimation was the overlapping of cotton bolls in the captured 2-D UAV images, which could be addressed by collection of 3-D images in the future. Linear regression analysis results indicated that both boll count and candidate area are the potential predictors of the lint yield. However, boll count was found to be a better predictor of lint yield than the candidate area. Overall, statistical evaluation and validation metrics obtained in this study suggest that the proposed cotton boll candidate recognition and boll count methods for UAV images could potentially lead to more effective and efficient evaluation and management of experimental plots or fields by researchers and producers.

#### **Declaration of Competing Interest**

The authors declare that they have no known competing financial interests or personal relationships that could have appeared to influence the work reported in this paper.

#### Data availability

Data will be made available on request.

#### Acknowledgements

We gratefully acknowledge the funding support provided by Cotton Incorporated for this study. Partial funding for this study was also provided by the Ogallala Aquifer Program, a consortium between USDA Agricultural Research Service, West Texas A&M University, Texas Tech University, Texas AgriLife Research, Texas AgriLife Extension Service and Kansas State University.

#### References

- J.S. Aber, I. Marzolff, J. Ries, Small-Format Aerial photography: Principles, Techniques and Geoscience Applications, Elsevier, 2010.
- [2] J.P. Bordovsky, J.T. Mustian, G.L. Ritchie, K.L. Lewis, Cotton irrigation timing with variable seasonal irrigation capacities in the Texas south plains, Appl. Eng. Agric. 31 (2015) 883–897.
- [3] A. Chang, J. Jung, M.M. Maeda, J. Landivar, Crop height monitoring with digital imagery from Unmanned Aerial System (UAS), Comput. Electron. Agric. 141 (2017) 232–237.
- [4] C. Cortes, V. Vapnik, Support-vector networks, Mach. Learn. 20 (1995) 273-297.
- [5] P. DeLaune, P. Mubvumba, Winter cover crop production and water use in Southern Great Plains cotton, Agron. J. 112 (2020) 1943–1951.
- [6] P. DeLaune, P. Mubvumba, Y. Fan, S. Bevers, Cover crop impact on irrigated cotton yield and net return in the Southern Great Plains, Agron. J. 112 (2020) 1049–1056.
- [7] Drucker H., Burges C.J.C., Kaufman L., Smola A., Vapnik V. 1997. Support vector regression machines. In: Mozer M.C., Jordan M.I., and Petsche T. (Eds.), Advances in Neural Information Processing Systems 9, MIT Press, Cambridge, MA, pp. 1551161.
- [8] J.J. Heitholt, Cotton boll retention and its relationship to lint yield, Crop Sci. 33 (1993) 486–490.
- [9] S.K. Himanshu, S. Ale, J.P. Bordovsky, J. Kim, S. Samanta, N. Omani, E.M. Barnes, Assessing the impacts of irrigation termination periods on cotton productivity under strategic deficit irrigation regimes, Sci. Rep. 11 (2021) 1–16.
- [10] S.K. Himanshu, Y. Fan, S. Ale, J. Bordovsky, Simulated efficient growth-stage-based deficit irrigation strategies for maximizing cotton yield, crop water productivity and net returns, Agric. Water Manag. 250 (2021), 106840.
- [11] J. Jung, M. Maeda, A. Chang, J. Landivar, J. Yeom, J. McGinty, Unmanned aerial system assisted framework for the selection of high yielding cotton genotypes, Comput. Electron. Agric. 152 (2018) 74–81.
- [12] F. Kurtulmus, W.S. Lee, A. Vardar, Immature peach detection in colour images acquired in natural illumination conditions using statistical classifiers and neural network, Precis. Agric. 15 (2014) 57–79.
- [13] D. Li, Y. Miao, C.J. Ransom, G.M. Bean, N.R. Kitchen, F.G. Ferna' ndez, J.E. Sawyer, J.J. Camberato, P.R. Carter, R.B. Ferguson, Corn nitrogen nutrition index prediction improved by integrating genetic, environmental, and management factors with active canopy sensing using machine learning, Remote Sens. 14 (2022) 304
- [14] Y. Li, Z. Cao, H. Lu, Y. Xiao, Y. Zhu, A.B. Cremers, In-field cotton detection via region-based semantic image segmentation, Comput. Electron. Agric. 127 (2016) 475–486.
- [15] G. Mountrakis, J. Im, C. Ogole, Support vector machines in remote sensing: a review, ISPRS J. Photogramm. Remote Sens. 66 (2011) 247–259.
- [16] N. Otsu, A threshold selection method from gray-level histograms, IEEE Trans. Syst. Man Cybern. 9 (1979) 62–66.
- [17] L. Prado Osco, A.P. Marques Ramos, D. Roberto Pereira, E´. Akemi Saito Moriya, N. Nobuhiro Imai, E. Takashi Matsubara, N. Estrabis, M. de Souza, J. Marcato Junior, W.N. Gonçalves, Predicting canopy nitrogen content in citrus-trees using random forest algorithm associated to spectral vegetation indices from UAV-imagery, Remote Sens. 11 (2019) 2925.

- [18] G. Rouze, H. Neely, C. Morgan, W. Kustas, M. Wiethorn, Evaluating unoccupied aerial systems (UAS) imagery as an alternative tool towards cotton-based management zones, Precis. Agric. 22 (2021) 1861–1889.
- [19] S. Sankaran, L.R. Khot, A.H. Carter, Field-based crop phenotyping: multispectral aerial imaging for evaluation of winter wheat emergence and spring stand, Comput. Electron. Agric. 118 (2015) 372–379.
- [20] Y. Shi, J.A. Thomasson, S.C. Murray, N.A. Pugh, W.L. Rooney, S. Shafian, N. Rajan, G. Rouze, C.L. Morgan, H.L. Neely, Unmanned aerial vehicles for high-throughput phenotyping and agronomic research, PLoS ONE 11 (2016), e0159781.
- [21] A.J. Smola, B. Scho "lkopf, A tutorial on support vector regression, Stat. Comput. 14 (2004) 199–222.
- [22] J.V. Stafford, Implementing precision agriculture in the 21st century, J. Agric. Eng. Res. 76 (2000) 267–275.
- [23] S. Sun, C. Li, A.H. Paterson, P.W. Chee, J.S. Robertson, Image processing algorithms for infield single cotton boll counting and yield prediction, Comput. Electron. Agric. 166 (2019), 104976.

- [24] Y. Tian, Y.P. Xu, G. Wang, Agricultural drought prediction using climate indices based on support vector regression in Xiangjiang River basin, Sci. Total Environ. 622 (2018) 710-720.
- [25] Wells, R., Meredith, W., 1984. Comparative growth of obsolete and modern cultivars. II. Reproductive dry matter partitioning nal References.
- [26] K. Yamamoto, W. Guo, Y. Yoshioka, S. Ninomiya, On plant detection of intact tomato fruits using image analysis and machine learning methods, Sensors 14 (2014) 12191–12206.
- [27] J. Yeom, J. Jung, A. Chang, M. Maeda, J. Landivar, Automated open cotton boll detection for yield estimation using unmanned aircraft vehicle (UAV) data, Remote Sens. 10 (2018) 1895.
- [28] H. Zha, Y. Miao, T. Wang, Y. Li, J. Zhang, W. Sun, Z. Feng, K. Kusnierek, Improving unmanned aerial vehicle remote sensing-based rice nitrogen nutrition index prediction with machine learning, Remote Sens. 12 (2020) 215.
- [29] C. Zhang, J.M. Kovacs, The application of small unmanned aerial systems for precision agriculture: a review, Precis. Agric. 13 (2012) 693–712.